Correlation of MLCTs of Group 7 *fac*-[M(CO)₃]⁺ Complexes (M = Mn, Re) with Bipyridine, Pyridinylpyrazine, Azopyridine, and Pyridin-2-ylmethanimine Type Ligands for Rational photoCORM Design

Emmanuel Kottelat,[a] Fiorella Lucarini,[a] Aurelien Crochet,[a] Albert Ruggi,[a] and Fabio Zobi*[a]

Abstract: A mathematical correlation of the MLCT absorption maxima of structurally related *fac*-[M(CO)₃L₂Br] complexes (M = Mn, Re; L₂ = bidentate ligand) is obtained by the comparison of a total of 50 species bearing bipyridine, pyridinylpyrazine, azopyridine and pyridin-2-ylmethanimine L₂ type ligands. The empirical relationship is first derived by the initial comparison of the MLCT absorption maxima of 26 previously published complexes and subsequently used to predict the same absorption value of 24 other species. In order to check the validity of the prediction, several new complexes were prepared. These were spectroscopically characterized and, where possible, their X-ray solid-state structure elucidated. The initial mathematical correlation allowed to predict MLCT absorption maxima of the unknown species with an average discrepancy of 12 nm. The relationship was subsequently refined to an average error of 6 nm with following derived formula $^{Calc}Mn_{MLCT} = (^{Obs}Re^{MLCT}/0.88) - 15.1$ (where $^{Calc}Mn_{MLCT}$ = predicted values of Mn complexes MLCT and $^{Obs}Re^{MLCT}$ = experimentally observed MLCT transitions of Re complexes). The correlation and the formula, the significance of which are discussed, may prove useful in the long run for the rational design of Mn-based photoCORMs starting from known data of widely investigated *fac*-[Re(CO)₃L₂Br] complexes.

Introduction

CO-releasing molecules (CORMs) are an established class of compounds that exploit the now well-known cytoprotective and homeostatic properties of carbon monoxide for medical applications. A challenge in the development of such molecules resides in the fact that the starting time of action of the molecules can be particularly difficult to influence. Methods to initiate controlled CO release rely on enzymatic,[1] electromagnetic heating,[2] pH and oxidation-dependent activation.[3] Light triggered release of CO is another convenient approach to work with CORMs because of the on-off feedback control it offers. When light is employed for the activation of these pro-drugs, the compounds are consensually referred as photoCORMs and undoubtedly *fac*-[Mn(CO)₃]⁺-based photoCORMs are the most commonly encountered in the scientific literature. The vast majority of photoCORMs is activated with wavelengths in the UV region of the electromagnetic spectrum but a shift towards the red region is desirable to achieve deeper skin penetration (e.g. for sub-cutaneous applications of the molecules) and to avoid the dangerous effects of UV light on living tissues.[4]

It remains however, very difficult to predict the wavelength of photo activation of new *fac*-[Mn(CO)₃]⁺-based photoCORMs. In fact, visible and infrared light-activated photoCORMs represent to date only a small fraction of all reported molecules.[5] The conceptual chemical framework for the synthesis of these species relies on modifications of the inner- and outer-coordination sphere of the metal ion in such a way as to finely tune the energy gap of the orbitals involved in the lowest energy electronic transition.[6] This is almost invariably a MLCT transition involving a HOMO of predominantly metal character and a LUMO mainly localized on the aromatic bidentate ligand (most often a polypyridyl ligand). This electronic transition has the crucial effect of reducing metal to ligand π-backbonding, hence destabilizing the M–CO bond, and leading to the liberation of CO in its gaseous form.

These chemical approaches enabled several authors to realize *fac*-[Mn(CO)₃]⁺-based photoCORMs with red-shifted MLCT transitions. Moreover, similar effects have been obtained by applying the same strategy to the corresponding Re derivatives, although in such cases it was observed that the presence of a strong MLCT transition in the visible region of the electromagnetic spectrum is not a sufficient prerequisite to activate *fac*-[Re(CO)₃]⁺-based photoCORMs towards CO release. While some examples have been reported,[7] the number of Re-based photoCORMs is marginal compared to the Mn-based ones. This difference is understood in terms of spin-orbit coupling (prominent in heavy metals) which promotes intersystem crossing to

[a] *Department of Chemistry, Faculty of Sciences, University of Fribourg, Chemin de Musée 9, 1700 Fribourg, Switzerland*
E-mail: fabio.zobi@unifr.ch
http://www3.unifr.ch/chem/en/research/groups/zobi/

the triplet [3]MLCT state in Re species thus stabilizing the M–CO bond.[8] Nevertheless, complexes of the *fac*-[Re(CO)$_3$]$^+$ core are extensively investigated for their use in e.g. catalysis,[9] imaging,[10] or cancer therapy,[11] and a large body of spectroscopic data is available in literature.

Given the structural and electronic similarities of *fac*-[M(CO)$_3$]$^+$ complexes of Re and Mn and the wealth of spectroscopic information of Re species, we wondered if the latter could not be exploited as a blueprint for the rational design of tri-carbonyl Mn-based photoCORMs. Relative effects of first row vs. third row transition metal ions in CO photorelease were partially discussed before[12] and it was shown by DFT calculations that the same orbitals are involved in the MLCT transition of equivalent complexes of the two metal ions.[6b,13] The difference being in the energy separation of the orbitals which, as expected, is greater for Re. With this theoretical basis, the starting hypothesis of this investigation was to assume that *fac*-[Re(CO)$_3$L$_2$Br] complexes behave spectroscopically in a related fashion to the analogous *fac*-[Mn(CO)$_3$L$_2$Br] species with the same bidentate L$_2$ ligand in identical conditions. This assumption is corroborated not only by logical chemical intuition but empirically also by a survey of the literature data.[6a,6b,13,14] Empirical correlations of electrochemical[15] and vibrational[16] parameters of Mn and Re complexes have been already reported. However, mathematical models correlating the light absorption properties for this class of complexes have never been established. Such a model could play an important role in the rational design of new photoCORMs. Moreover, since Re complexes are usually more stable than their Mn counterparts, the application of this model would simplify the synthetic efforts. In fact, the possibility of predicting *a priori* the MLCT transition of the target molecules is certainly an advantage for the rational design of photoCORMs.

In this contribution we have precisely investigated this possibility and we show that a mathematical correlation of the MLCT absorption maxima of structurally related *fac*-[M(CO)$_3$L$_2$Br] complexes (M = Mn, Re; L$_2$ = bidentate ligand) can be derived from the comparison of these species. The empirical mathematical relationship described in the following pages was first derived by the comparison of previously published complexes and subsequently used to predict the same absorption value of other species. To check the validity of the prediction several new complexes were prepared and are herein reported. The significance of the correlation is finally discussed.

Results and Discussion

Data Selection and First Correlation

In order to gather enough data for a statistically significant comparison, we began our study with a literature research of structurally related *fac*-[M(CO)$_3$L$_2$Br] complexes (M = Mn, Re; L$_2$ = bidentate ligand). We restricted our selection to pairs of complexes with identical coordination spheres and (where possible) whose MLCT absorption maxima were tabulated. It is worth to mention that the determination of MLCT transition is not always trivial, particularly for Re species whose MLCT bands

often appear as shoulders of the stronger ligand π–π* transitions. This initial search led to the selection of thirteen pairs of Re- and Mn-based compounds (**1**–**26**, Figure 1). The MLCT absorption maxima of these species are given in Table 1 and
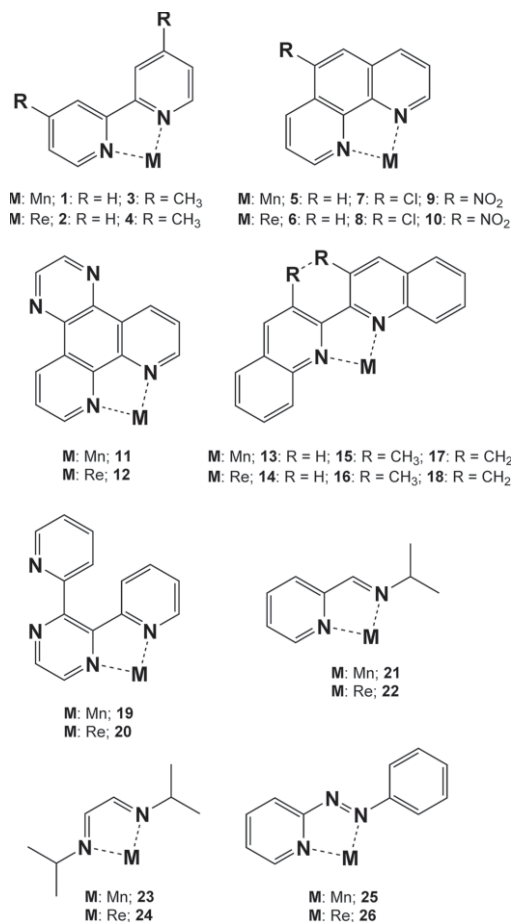

Figure 1. Molecular structures of species **1–26**. M = *fac*-[M(CO)$_3$Br] with either Mn or Re.

Table 1. MLCT absorption maxima of complexes **1–26**.

Mn species	MLCT [nm]	Re species	MLCT [nm]	Δ [nm][h]
1[14]	430[a]	**2**[14]	370[a]	60
3[17]	420[c]	**4**[18]	380[d]	40
5[14]	430[a]	**6**[14]	370[b]	60
7[19]	426[d]	**8**[19]	375[d]	51
9[19]	430[d]	**10**[19]	388[d]	42
11[20]	430[a]	**12**[14]	375[b]	55
13[21]	495[c]	**14**[22]	452[c]	43
	508[g]		464[g]	44
15[22]	452[e]	**16**[22]	418[e]	34
	473[g]		430[g]	43
17[22]	497[e]	**18**[22]	450[e]	47
	517[g]		465[g]	52
19[17]	460[a]	**20**[36]	415[b]	45
21[23]	452[c]	**22**[24]	396[f]	56
23[25]	485[c]	**24**[24]	435[c]	50
25[13]	586[d]	**26**[13]	530[d]	56

[a] CH$_2$Cl$_2$. [b] DMF. [c] THF. [d] CH$_3$CN. [e] CHCl$_3$. [f] Butyronitrile, and [g] Toluene as solvent. [h] Δ = Mn$_{MLCT}$ – Re^{MLCT}.
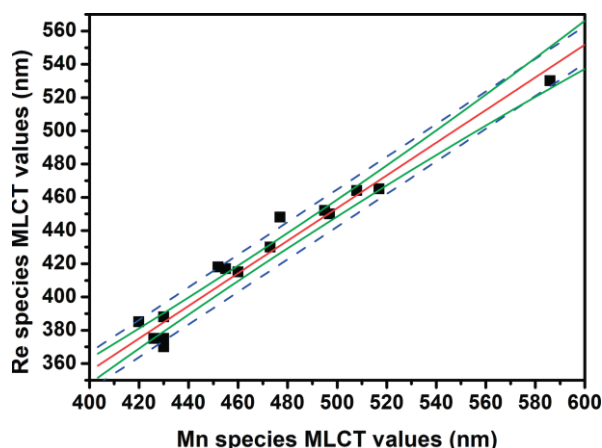
2

Figure 2. Plot of observed MLCT absorption maxima of *fac*-[Mn(CO)₃L₂Br] complexes against the same value of the corresponding *fac*-[Re(CO)₃L₂Br] complexes (species **1–26**). Red line = linear fitting (R² = 0.96); green lines = 95 % confidence interval; blue lines = 95 % prediction interval.

plotted in Figure 2. According to the best linear fit through the 16 points plotted in Figure 2, the following equation is derived for the MLCT correlation of *fac*-[M(CO)₃L₂Br] complexes:

$$^{Obs}Re^{MLCT} [nm] = (0.98 \pm 0.05) \, ^{Obs}Mn_{MLCT} [nm] - (37.4 \pm 26.0)$$
$$(R^2 = 0.96)$$

(where $^{Obs}Re^{MLCT}$ and $^{Obs}Mn_{MLCT}$ = experimentally observed MLCT transitions of Re and Mn complexes, in nm). UV/Visible absorption spectra are largely dependent on the medium in which they are recorded and solvatochromic effects are expected to influence the correlation. Unfortunately, for each pair of compounds different authors report data in different solvents. No correction was made to account for variables like the pH, polarity, dielectric constants, or viscosity of the medium. The analysis shows that the MLCT absorption maxima of four pair of complexes (**1/2**, **5/6**, **15/16** measured in CHCl₃ and **23/24**) are outside the 95 % confidence interval (CI). Because CI is a type of interval estimate that might contain the true value of an unknown population parameter, we excluded these points and recalculated the equation above: Equation (1).

$$^{Obs}Re^{MLCT} [nm] = (0.94 \pm 0.04) \, ^{Obs}Mn_{MLCT} [nm] - (17.4 \pm 18.0)$$
$$(R^2 = 0.98) \tag{1}$$

Some scattering is observed particularly in the more energetic transitions of complexes bearing bipyridine type ligands but the correlation between observed MLCT absorption maxima of structurally related *fac*-[M(CO)₃L₂Br] complexes shows a good linearity, as proved by the value of R² parameter which is very close to the unit (R² = 0.98).

Having established a first correlation between the MLCT absorption maxima of related *fac*-[M(CO)₃L₂Br] complexes, we proceeded to its validation and refinement. To this end, we sought to predict via Equation (1) the MLCT absorption values of a) species that were not included in the initial correlation and b) previously unknown complexes. Six Re complexes (**30–38** and **46**, Figure 3) were then synthesized in order to compare them with corresponding Mn compounds published in literature. For the same reason, Mn complex **39** was also prepared

along with molecule pairs **41–44** and **47–50** (Figure 3). Finally complex **28**, previously published by the group of Alberto,[14] was resynthesized in order to obtain its electronic UV/Visible spectrum in the same solvent of the corresponding Mn species published by our group.[6a]
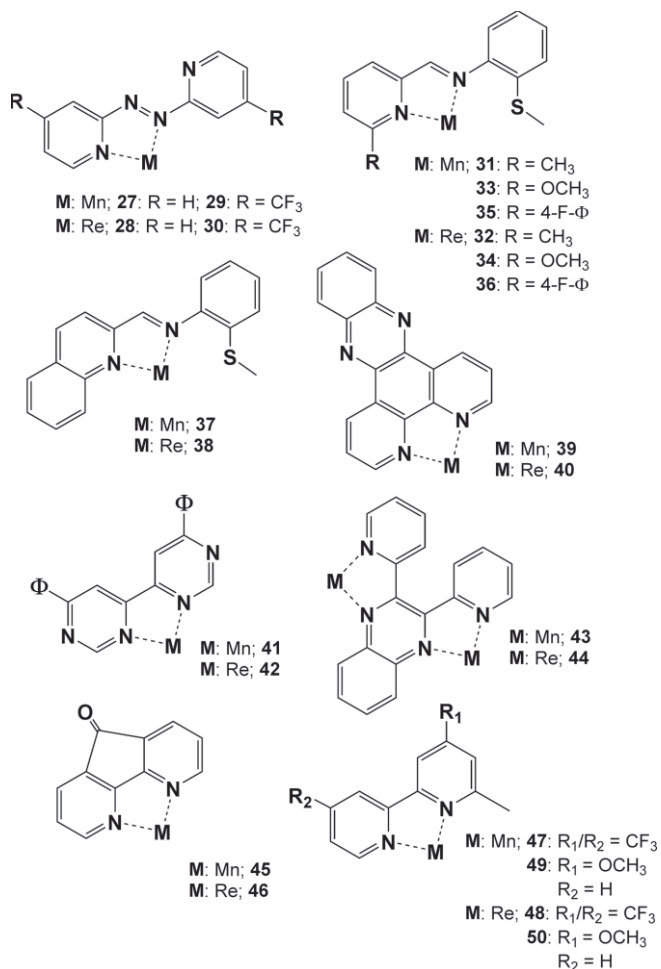

Figure 3. Molecular structures of species **27–50**. M = *fac*-[M(CO)₃Br] with either Mn or Re; Φ = phenyl.

Synthesis and Characterization

Re complexes **30–38** and **42–50** were prepared by reaction of the [Et₄N]₂*fac*-[Re(CO)₃Br₃] salt with the relevant L₂ ligands which were in turn prepared according to reported procedures (see experimental section for details). All new species were characterized via standard techniques and their purity confirmed via elemental analysis. ¹H-NMR spectra showed pure diamagnetic compounds, according to the symmetry given by the facially arranged COs and low-spin d6 nature of the metal ion. IR spectroscopy analysis was in accordance with the typical tricarbonyl vibration pattern. Of this complex series, crystals suitable for X-ray diffraction analysis were obtained for eight species. Crystallographic details are presented in Table 2, spectroscopic data are listed in Table 3 while structural parameters are given in the Supporting Information.

3

Table 2. Crystallographic details for complexes **32**, **34**, **36**, **38**, **44**, **46**, **49**, and **50**.

	32	**34**	**36**	**38**	**44**	**46**	**49**	**50**
Formula	$C_{17}H_{14}BrN_2O_3ReS$	$C_{17}H_{14}BrN_2O_4ReS$	$C_{22}H_{15}BrFN_2O_3ReS$	$C_{20}H_{14}BrN_2O_3ReS$	$C_{24}H_{12}Br_2N_4O_6Re_2$	$C_{14}H_6BrN_2O_4Re$	$C_{15}H_{12}BrMnN_2O_4$	$C_{15}H_{12}BrN_2O_4Re$
M_W	592.48	608.48	672.54	628.51	984.60	532.32	419.11	550.38
T [K]	250(2)	250(2)	250(2)	250(2)	200(2)	293(2)	250(2)	250(2)
Lattice	triclinic	triclinic	monoclinic	monoclinic	monoclinic	monoclinic	monoclinic	triclinic
Space group	$P1$	$P1$	$P2_1/n$	$P2_1/n$	$C2/c$	$P2_1/n$	$P2_1/n$	$P1$
Z	2	2	4	4	4	4	4	2
a [Å]	7.6734(5)	7.7208(10)	7.9346(4)	10.0632(4)	17.6909(8)	6.5359(7)	9.0940(5)	7.9055(10)
b [Å]	7.7388(5)	7.8806(10)	21.9827(11)	11.6027(3)	24.7765(7)	16.7815(19)	15.1304(9)	8.3868(10)
c [Å]	17.3622(12)	17.915(2)	12.5942(6)	17.3107(8)	6.8265(2)	13.2352(16)	11.5589(7)	12.1769(17)
α [°]	83.703(5)	87.252(10)	90	90	90	90	90	93.574(9)
β [°]	86.496(6)	79.557(10)	96.199(4)	99.629(4)	99.689(4)	100.162(9)	99.670(5)	93.489(10)
γ [°]	65.608(5)	63.761(9)	90	90	90	90	90	90.658(10)
V [Å^3]	933.183	960.875	2183.89	1992.73	2949.5	1428.89	1567.86	804.19
d_{calcd} [g/cm^3]	2.109	2.103	2.045	2.095	2.217	2.474	1.776	2.273
R_1, wR_2	0.0237, 0.0593	0.0193, 0.0415	0.032, 0.0732	0.0219, 0.0500	0.0419, 0.1266	0.1298, 0.3060	0.0397, 0.1093	0.0793, 0.2600

Table 3. MLCT absorption maxima[a] of complexes **27–50**.

Mn species	MLCT [nm] observed	MLCT [nm] predicted[b]	Δ [nm][c]	Re species	MLCT [nm] observed	MLCT [nm] predicted[b]	Δ [nm][c]
27[6a]	630	626.0	4.0	**28**[14]	571	574.8	3.8
29[6a]	678	667.4	10.6	**30**	610	619.9	9.9
31[26a]	488	460.0	28.0	**32**	415	441.3	26.3
33[26a]	498	491.9	6.1	**34**	445	450.7	5.7
35[26a]	497	495.1	1.9	**36**	448	449.8	1.8
37[26b]	535	529.1	5.9	**38**	480	485.5	5.5
39	430	444.0	14.0	**40**[14]	400	386.8	13.2
41	512	529.1	17.1	**42**	480	463.9	16.1
43	573	596.2	23.2	**44**	543	521.2	21.8
45[20]	430	444.0	14.0	**46**	400	386.8	13.2
47	463	472.8	9.8	**48**	427	417.8	9.2
49	407	416.4	9.4	**50**	374	365.2	8.8

[a] CH$_2$Cl$_2$ as solvent. [b] According to Equation (1). [c] $\Delta = |M^{MLCT}_{pred.} - M^{MLCT}_{obs.}|$.
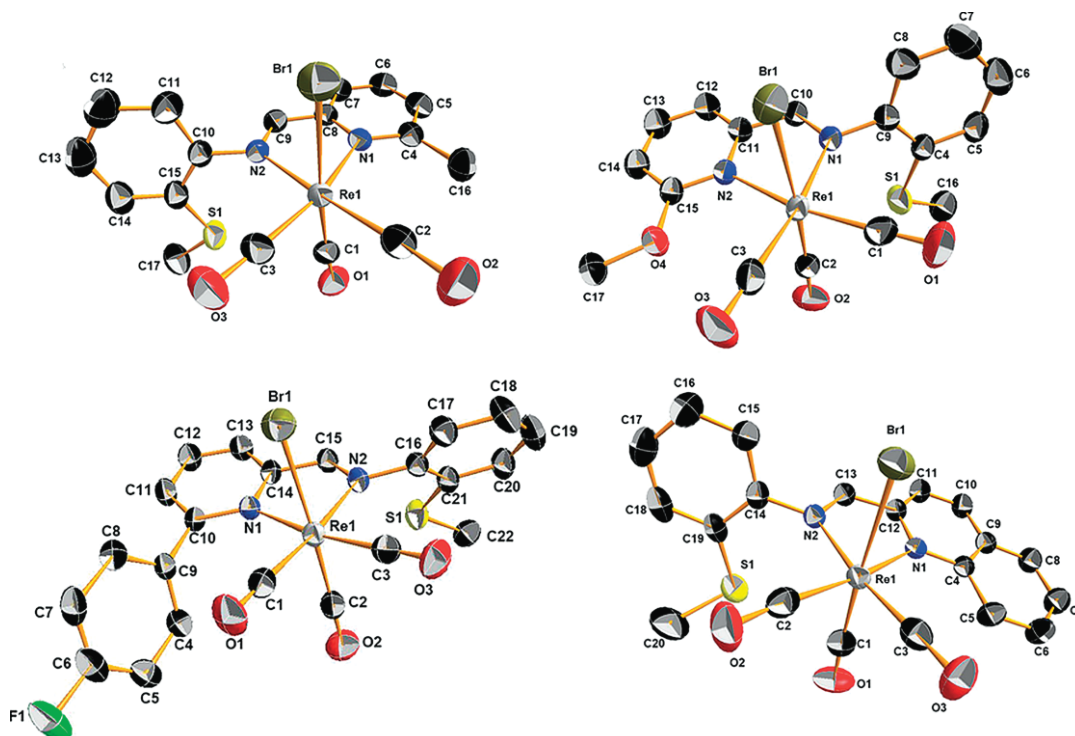

Figure 4. X-ray structures of: (top) species **32** (left) and **34;** (bottom) **36** (left) and **38**. Thermal ellipsoids set at a 30 % probability level. Hydrogen atoms are omitted for clarity.
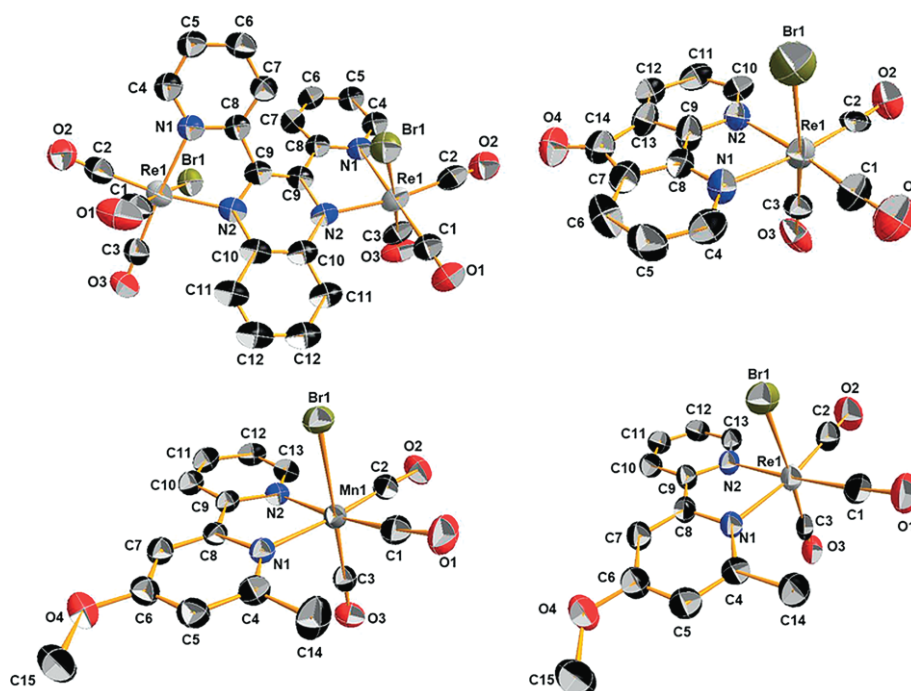
Figure 5. X-ray structures of (top) species **44** (left) and **46**, and (bottom) **49** (left) and **50**. Thermal ellipsoids set at a 30 % probability level. Hydrogen atoms are omitted for clarity.

Complexes **32** and **34** crystallized in a triclinic lattice and space group $P1$ whereas **36** and **38** were obtained in the monoclinic space group $P2_1/n$ (Figure 4). The four complexes present a distorted octahedral geometry with structural parameters similar to those of the analogous Mn-based complex.[26] Crystals of **44** were obtained by slow evaporation of an acetone solution (Figure 5). The molecule crystallized in a monoclinic lattice in the space group $C2/_c$. As predicted, two metallic centers are connected homotopically to each binding site of the ligand. Each fac-[Re(CO)$_3$]$^+$ unit is coordinated to both the pyrimidine and pyrazine sites of the ligands with one bromide ion as ancillary ligand. Crystals of compound **46**, **49** and **50** suitable for X-ray diffraction measurements were obtained by pentane diffusion into a CH$_2$Cl$_2$ solution (Figure 5). Complex **46** crystallized in the monoclinic space group $P2_1/n$, whereas compounds **49** and **50** in the monoclinic space group $P2_1/n$ and in the triclinic space group P1 respectively. The complexes exhibit a slightly distorted octahedral geometry but are not significantly different from the corresponding manganese complexes previously described.[20,27]

UV/Visible Electronic Spectroscopy and Correlation Validation and Refinement

Table 3 lists spectroscopic data of compounds **27–50** while Figure 6 shows selected absorption spectra of the same complexes. Mn species typically show MLCT bands at a wavelength of 430, 500–550 and 630 nm for complexes bearing bipyridines, pyridin-2-ylmethanimines and azopyridines respectively. For the corresponding Re complexes the wavelength required for same transitions is 30–50 nm higher. In order to validate the correlation shown in Figure 2, the measured MLCT absorption maxima
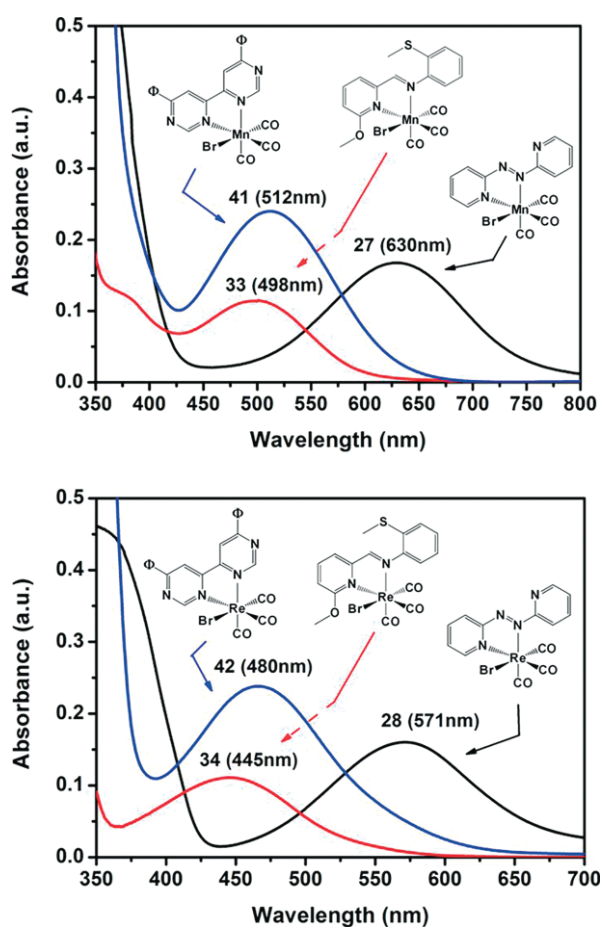

Figure 6. Selected absorption spectra of representative fac-[M(CO)$_3$L$_2$Br] complexes (M = Mn, top, M = Re, bottom) investigated in this study.

of a set of species of one of the metal congeners (e.g. Mn) were used to predict the position of the same transition for the other set of metal (e.g. Re) complexes according to Equation (1).

Thus, the MLCT absorption maxima of each metal ion were calculated starting from the observed absorbance of the corresponding congener (i.e. by using observed Re^{MLCT} to predict Mn_{MLCT} and vice versa). The results of this analysis are shown in Figure 7 where $^{Obs}M^{MLCT}$ and $^{Calc}M^{MLCT}$ absorption maxima for each metal ion are plotted. According to the fit through the 12 points plotted in Figure 7, $^{Obs}M^{MLCT}$ and $^{Calc}M^{MLCT}$ positions correlate linearly with R^2 values of 0.97.
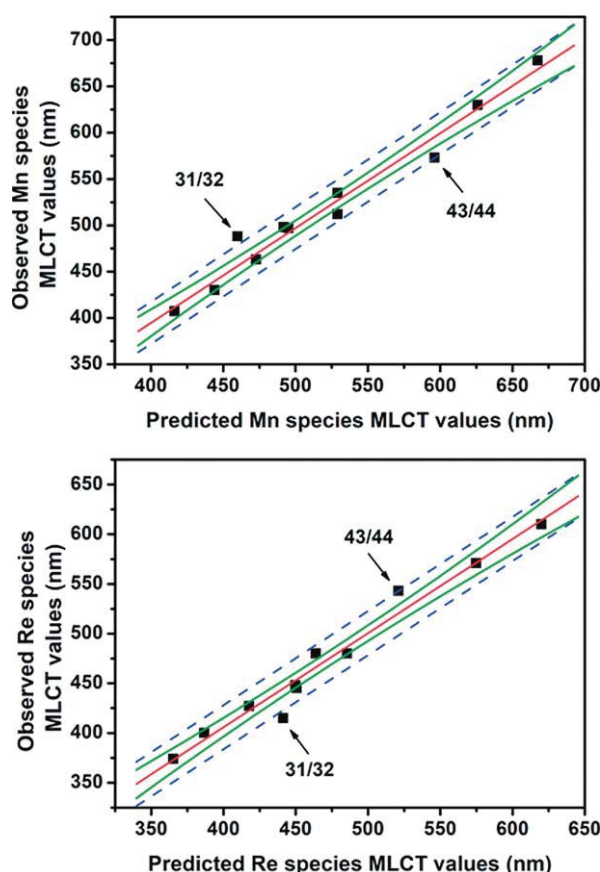
Figure 7. Plot of observed vs. predicted MLCT absorption maxima of *fac*-[M(CO)$_3$L$_2$Br] complexes (M = Mn, top, R^2 = 0.97; M = Re, bottom, R^2 = 0.97) according to Equation (1). Predicted MLCT absorption maxima for each metal ion were calculated starting from the observed absorbance values of the corresponding congener (i.e. using observed Re^{MLCT} to predict Mn_{MLCT} and vice versa). Red lines = linear fits; green lines = 95 % confidence interval; blue lines = 95 % prediction interval.

In both cases (i.e. whether predicting via (1) Mn values from Re data or vice versa) an average discrepancy of 12 nm is calculated between $^{Obs}M^{MLCT}$ and $^{Calc}M^{MLCT}$. The pair of complexes **31/32** and **43/44** (see Figure 3) lay out of line and the confidence interval, with a difference > 21 nm between the observed and predicted values. The former are complexes bearing a pyridin-2-ylmethanimines ligand. Lumsden has shown that such compounds (with Mn as central metal ion) undergo speciation in solution as a consequence of the thioether group re-

placing a *cis* CO ligand and thereby altering the coordination sphere of the metal center and the wavelength of the MLCT band.[26a] We believe, however, that it is rather unlikely that the same type of ligand substitution (i.e. CO replacement) takes place in stable *fac*-[Re(CO)$_3$Br] species. In fact, we found no such evidence via IR or NMR spectroscopy. The latter couple (i.e. **43/44**) is the only dimeric set of the entire 50 complexes series we have analyzed. Here perhaps electronic coupling between the metal centers may influence the metal-centered HOMO or ligand-centered LUMO energies to an extent not observable in mononuclear complexes. If these points are omitted, $^{Obs}M^{MLCT}$ and $^{Calc}M^{MLCT}$ positions correlate linearly with R^2 values of 0.99.

Having established the possibility of predicting via Equation (1) MLCT absorption values of species which were not included in the initial correlation, the latter was refined by including all 44 complexes in the analysis (i.e. 25–3 pair of complexes out of CI). Equation (1) was thus recalculated to:

$$^{Obs}Re^{MLCT} \text{ [nm]} = (0.89 \pm 0.02) \, ^{Obs}Mn_{MLCT} \text{ [nm]} + (7.8 \pm 11.2)$$
$$(R^2 = 0.99) \tag{2}$$

Equation (2) was subsequently used to derive $^{Calc}Mn_{MLCT}$ from tabulated $^{Obs}Re^{MLCT}$ absorption maxima and the former
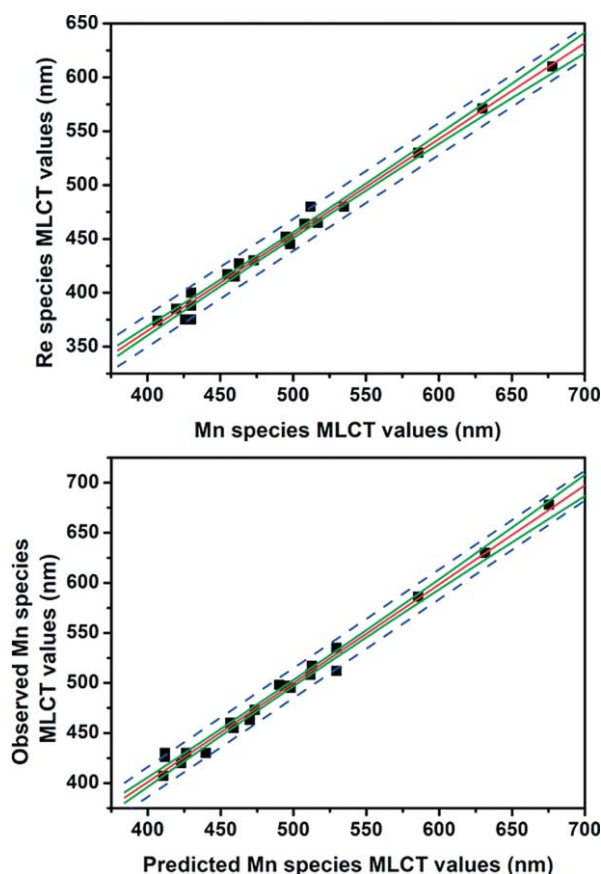
Figure 8. Top: plot of observed MLCT absorption maxima of *fac*-[Mn(CO)$_3$L$_2$Br] complexes against the same value of corresponding *fac*-[Re(CO)$_3$L$_2$Br] complexes (22 pairs of complexes, R^2 = 0.99). Bottom: plot of observed vs. predicted [according to Equation (4)] MLCT absorption maxima of *fac*-[Mn(CO)$_3$L$_2$Br] complexes (22 pairs of complexes, R^2 = 0.99). Red lines = linear fits; green lines = 95 % confidence interval; blue lines = 95 % prediction interval.

than the experimentally observed [Obs]Mn$_M$LCT data. The analysis gave:

$$^{Obs}Mn_MLCT \text{ [nm]} = (0.99 \pm 0.03)\ ^{Calc}Mn_MLCT \text{ [nm]} + (6.2 \pm 12.4)$$
$$(R^2 = 0.99) \hspace{3cm} (3)$$

Finally, [Obs]Mn$_M$LCT from Equation (3) was substituted in Equation (2) in order to directly relate experimentally observed MLCT transitions of Re complexes (i.e. [Obs]Re^{MLCT}) to [Calc]Mn$_M$LCT. The linear regression between the scalar dependent [Calc]Mn$_M$LCT variable and the independent [Obs]Re^{MLCT} variable finally gave the following relationship:

$$^{Calc}Mn_MLCT \text{ [nm]} = (^{Obs}Re^{MLCT} \text{ [nm]}/0.88 \pm 0.06) - 13.3 \pm 17.9$$
$$(R^2 = 0.99) \hspace{3cm} (4)$$

With Equation (4) the average discrepancy between [Calc]Mn$_M$LCT and [Obs]Mn$_M$LCT was further reduced to 6 nm (i.e. [Calc]Mn$_M$LCT = [Obs]Mn$_M$LCT ± 6 nm). Plots of this analysis are shown in Figure 8. All points calculated with (4) fall within the statistical 95 % prediction interval.

Significance of the Correlation

As mentioned in the introduction, the study described above was intended to derive a mathematical tool for the rational design of Mn-based photoCORMs starting from known spectroscopic data of widely investigated *fac*-[Re(CO)$_3$L$_2$Br] complexes. With Equation (4) this is now possible within an acceptable margin of error. Beyond the potential practical aspects of this study, some theoretical considerations may be discussed. MLCTs analyzed in this study involve formally excitation of an electron from a HOMO of predominantly metal character to a LUMO of predominantly L$_2$ ligand character. As such, the wavelength of MLCTs can be taken as a measure of the relative energy separation between the two orbitals (i.e. the HOMO-LUMO gap). The energetic separation between the HOMO and the LUMO is obviously greater for the third row Re ion and it originates fundamentally from: a) the greater radial extension of Re 5d orbitals (as compared to Mn 3d orbitals) which interact more strongly with L$_2$ ligand orbitals, b) the energetic separation ΔE between donor and acceptor atomic orbitals involved in bonding, and c) the overlap integral S between the two orbitals (and thus the metal-ligand bond length). There is clearly a strong interplay among the three factors in determining the final MO orbital energies. Given that we have compared *fac*-[M(CO)$_3$L$_2$Br] complexes with identical coordination spheres, the atomic orbital energies of the ligands can be considered as a constant, thus the HOMO-LUMO gap (and the energy associated with the MLCT wavelength) may be taken as dependent only of the metal atomic orbital energies. For our discussion, we will consider calculated orbital energies for the neutral metal atoms. These depend strongly on the configuration used to calculate the ground state, but since both metal ions analyzed are low spin d6 ions our assumption should give a coherent picture. If one considers only calculated orbital energies for the neutral metal atoms it is interesting to note that the 0.89 value of the slope correlating Mn$_M$LCT and Re^{MLCT} is approximately the same factor relating metal d-orbital energies for the neutral

metal atoms (i.e. –12.05 eV and –10.62 eV for Mn and Re respectively; 10.62/12.05 = 0.88).[28] We finally note in passing that theoretically one should be able to correlate MLCT energies with the electrochemical[15] (E$_L$) and infrared[16] (IR$_P$) parameters previously described (both of which are a measure of the electronic density on the central metal ion on octahedral complexes). In particular, given that MLCTs formally involve oxidation of the metal ion and reduction of the of L$_2$ ligand, a linear correlation should be observed with the E$_L$ parameters. Unfortunately, the limited number of ligands parametrized in the two models, and common to the study herein described does not permit to establish a quantitative correlation of our model with electrochemical and vibrational data.

Conclusions

Facial tricarbonyl Mn(I) species are known as photoactivatable CO releasing molecules (photoCORM). As a starting base for the rational design of Mn-based photoCORMs, a mathematical correlation of the MLCT absorption maxima of structurally related *fac*-[M(CO)$_3$L$_2$Br] complexes (M = Mn, Re; L$_2$ = bidentate ligand) was described in order to tentatively predict the MLCT absorption energies of manganese complexes from measured MLCT absorption maxima of analogous rhenium compounds with identical coordination ligand-spheres. The empirical relationship was determined for *fac*-[M(CO)$_3$L$_2$Br] species coordinated by bipyridine, pyridinylpyrazine, azopyridine and pyridin-2-ylmethanimine L$_2$ type ligands. To archive a statistically significant correlation, a total of 25 pairs of complexes were analyzed including several new complexes which were prepared to check the validity of the prediction. Formula (4) allows predicting MLCT absorption maxima of unknown Mn species with an average error of 6 nm. The correlation shows relatively high dispersion for points < 425 nm, thus one may tentatively posit the assumption that the correlation is valid mostly for compounds with MLCTs in the visible light region of the spectrum. While it is clear that the design of potentially valuable photoCORM cannot be reduced to a simple MLCT transition position, we believe that the possibility of predicting *a priori* specific characteristics of the molecules (i.e. in this case the wavelength of photoactivation) constitutes an important tool for the design of photoCORMs. Equation (4) may thus prove useful in the field as a guide for a preliminary check to evaluate if efforts directed towards synthesis of a new type of potential photoCORMs with specific required wavelengths of CO activation may be valuable or not, also in view of the higher stability of Re complexes with respect to their Mn analogues.

Experimental Section

Data Selection: The literature was searched for a large representative number of structurally identical complexes of the type *fac*-[M(CO)$_3$L$_2$L'] (M = Mn, Re) with the metal ion in a d6 configuration. Both monomeric and dimeric species with mono- (L') and bidentate (L$_2$) ligands were included in the pool. MLCT data were selected as reported by the authors and no solvent correction was applied to the reported values. Statistical analysis of confidence and prediction

intervals of the parameters were performed according to the procedure described by Bewik et al.[29] The Excel program (2016) was used to setup formula for statistical analysis and derive equations for the best linear fits. The Origin program (version 7.5) was used to plot data.

General Experimental Details: All chemicals and reagents were purchased from standard commercial sources, stored in accordance to the indications provided by the supplier and used as received. All the reactions, purifications and solution analysis involving Mn(I) species were carried out in the absence of light. Solid IR spectra were recorded on a Bruker Tensor 27 instrument. ESI-MS were recorded on a Bruker esquire HCT spectrometer, with methanol as solvent. ^{1}H-NMR were recorded on Bruker Avance III spectrometers operating at 400 or 500 MHz (as specified for each molecule). The corresponding ^{1}H shifts are reported relative to residual solvent protons. UV/Vis spectroscopy was performed using a Jasco V-730 spectrophotometer and data treated with the SpectraManager software. The λ_{max} of the MLCT transitions of newly synthesized complexes were chosen by calculating the first derivative of the absorption curve and selecting the numerical value where the derivative is 0. Elemental analyses (EA) were performed on a Leco CHNS-932 elemental analyzer. Single crystal diffraction collections were done on Stoe IPDS2 diffractometer (Mo$K_{\alpha 1}$ (λ = 0.71073 Å)) equipped with a cryostat from Oxford Cryosystems. The structure were solved with the ShelXT structure solution program[30] using Intrinsic Phasing and refined with the ShelXL refinement package[31] using least-squares minimization.

CCDC 1877322 (for **34**), 1877323 (for **32**), 1877324 (for **36**), 1877325 (for **46**), 1877326 (for **44**), 1877327 (for **38**), 1877422 (for **49**), and 1877423 (for **50**) contain the supplementary crystallographic data for this paper. These data can be obtained free of charge from The Cambridge Crystallographic Data Centre.

Synthesis of Ligands and Metal Complexes

fac-[Re(CO)$_3$L$_2$Br] L$_2$ = (1,2-Bis(4-(trifluoromethyl)pyridin-2-yl)-diazene) (30): The L$_2$ ligand was prepared according to literature.[6a] A total of 39 mg (0.05 mmol) of [Et$_4$N]$_2$ *fac*-[Re(CO)$_3$Br$_3$] were dissolved in 10 mL of H$_2$O. Then, 20 mg (0.06 mmol, 1.1 equiv.) of L$_2$ in 1 mL of ethanol were added dropwise under nitrogen. The reaction mixture was then stirred at room temperature for 4 h under nitrogen, until a green precipitate was formed. The compound was filtered, and a purified by column chromatography (SiO$_2$) using CH$_2$Cl$_2$/MeOH + NH$_3$ 10 % 98:2 as eluent. The expected compound was the first blue product to elute. The fraction was collected, dried and analyzed. Yield: 13 mg (27 %). Elemental Anal. Calcd. for C$_{15}$H$_6$BrF$_6$N$_4$O$_3$Re: C 26.88 %, H 0.90 %, N 8.36 %. Found: C 27.03 %, H 1.00 %, N 8.97 %. ^{1}H-NMR (500 MHz, CD$_2$Cl$_2$): δ (ppm) = 7.94–7.90 (m, 2H), 8.62 (s, 1H), 9.00 (s, 1H), 9.03 (d, J = 5.14 Hz, 1H), 9.35 (d, J = 5.80 Hz, 1H). IR (KBr pellet): $\nu_{C \equiv O}$ = 2032 cm^{-1}, 1923 cm^{-1}. MLCT band (CH$_2$Cl$_2$) [ε (M^{-1} cm^{-1})]: 610 nm (4459). ESI-MS analysis (positive mode) m/z = 591.1 [M − Br]$^+$.

Complexes **32**–**36** and their respective ligands L$_2$ were prepared according to the procedure described in literature[26a] for the equivalent Mn complexes with small variations. Generally: the [Et$_4$N]$_2$ *fac*-[Re(CO)$_3$Br$_3$] salt and the L$_2$ ligand were dissolved in separate CH$_2$Cl$_2$ solutions. L$_2$ was then added dropwise under nitrogen to the Re solution. The reaction mixture was then stirred under nitrogen at room temperature overnight. At the end of the reaction, pentane was carefully layered on top of the solution and the mixture was

allowed to stand until crystals of **32**–**36** appeared. These were then filtered, dried and analysed. Single crystals suitable for X-ray diffraction analysis were grown by slow diffusion of pentane into a CH$_2$Cl$_2$ solution of the complex.

fac-[Re(CO)$_3$L$_2$Br] L$_2$ = (N-((6-Methylpyridin-2-yl)methylene)-2-(methylthio)aniline) (32): 219 mg (0.284 mmol) of [Et$_4$N]$_2$ *fac*-[Re(CO)$_3$Br$_3$] in 10 mL of CH$_2$Cl$_2$; 67 mg (0.275 mmol, 0.9 equiv.) of L$_2$ in 10 mL of CH$_2$Cl$_2$. Yield: 98 mg (58 %). Elemental Anal. Calcd. for C$_{17}$H$_{14}$BrN$_2$O$_3$ReS: C 34.46 %, H 2.38 %, N 4.73 %. Found: C 34.55 %, H 2.42 %, N 4.70 %. ^{1}H-NMR (400 MHz, CD$_2$Cl$_2$): δ (ppm) = 2.53 (s, 3H), 3.06 (s, 3H), 7.32 (t, J = 7.58 Hz, 1H), 7.39 (t, J = 7.58 Hz, 1H), 7.45 (d, J = 7.95 Hz, 1H), 7.64 (d, J = 7.95 Hz, 1H), 7.67 (d, J = 7.66 Hz, 1H), 7.83 (d, J = 7.65 Hz, 1H), 7.97 (t, J = 7.66 Hz, 1H), 8.75 (s, 1H). IR (KBr pellet): $\nu_{C \equiv O}$ = 2014 cm^{-1}, 1881 cm^{-1}. MLCT band (CH$_2$Cl$_2$) [ε (M^{-1} cm^{-1})]: 413 nm (1865). ESI-MS analysis (positive mode) m/z = 513.1 [M − Br]$^+$.

fac-[Re(CO)$_3$L$_2$Br] L$_2$ = (N-((6-Methoxypyridin-2-yl)methylene)-2-(methylthio)aniline) (34): 219 mg (0.284 mmol) of [Et$_4$N]$_2$ *fac*-[Re(CO)$_3$Br$_3$] in 10 mL of CH$_2$Cl$_2$; 71 mg (0.275 mmol, 0.9 equiv.) of L$_2$ in 10 mL of CH$_2$Cl$_2$. Yield: 87 mg (50 %). Elemental Anal. Calcd. for C$_{17}$H$_{14}$BrN$_2$O$_4$ReS: C 33.56 %, H 2.32 %, N 4.60 %. Found: C 33.98 %, H 2.36 %, N 4.51 %. ^{1}H-NMR (400 MHz, CD$_2$Cl$_2$): δ (ppm) = 2.51 (s, 3H), 4.19 (s, 3H), 7.18 (d, J = 8.63 Hz, 1H), 7.31 (t, J = 7.55 Hz, 1H), 7.37 (dt, J = 7.62 Hz, 1H), 7.44 (d, J = 7.92 Hz, 1H), 7.65 (d, J = 7.38 Hz, 1H), 7.69 (d, J = 7.76 Hz, 1H), 8.08 (t, J = 8.02 Hz, 1H), 8.72 (s, 1H). IR (KBr pellet): $\nu_{C \equiv O}$ = 2014 cm^{-1}, 1877 cm^{-1}. MLCT band (CH$_2$Cl$_2$) [ε (M^{-1} cm^{-1})]: 445 nm (2272). ESI-MS analysis (positive mode) m/z = 528.9 [M − Br]$^+$.

fac-[Re(CO)$_3$L$_2$Br] L$_2$ = (N-((6-(4-Fluorophenyl)pyridin-2-yl)methylene)-2-(methylthio)aniline) (36): 219 mg (0.284 mmol) of [Et$_4$N]$_2$ *fac*-[Re(CO)$_3$Br$_3$] in 10 mL of CH$_2$Cl$_2$; 88 mg (0.275 mmol, 0.9 equiv.) of L$_2$ in 10 mL of CH$_2$Cl$_2$. Yield: 119 mg (62 %). Elemental Anal. Calcd. for C$_{22}$H$_{15}$BrFN$_2$O$_3$ReS: C 39.29 %, H 2.25 %, N 4.17 %. Found: C 38.30 %, H 2.26 %, N 4.01 %. ^{1}H-NMR (400 MHz, CD$_2$Cl$_2$): δ (ppm) = 2.54 (s, 3H), 7.26–7.33 (m, 4H), 7.39 (t, J = 7.61 Hz, 1H), 7.45 (d, J = 8.03 Hz, 1H), 7.62 (d, J = 7.72 Hz, 2H), 7.73 (d, J = 7.85 Hz, 1H), 8.05 (d, J = 7.61 Hz, 1H), 8.15 (t, J = 7.71 Hz, 1H), 8.96 (s, 1H). IR (KBr pellet): $\nu_{C \equiv O}$ = 2019 cm^{-1}, 1934 cm^{-1}, 1897 cm^{-1}. MLCT band (CH$_2$Cl$_2$) [ε (M^{-1} cm^{-1})]: 390 nm (1336). ESI-MS analysis (positive mode) m/z = 593.1 [M − Br]$^+$.

fac-[Re(CO)$_3$L$_2$Br] L$_2$ = (2-(Methylthio)-N-(quinolin-2-ylmethylene)aniline) (38): The L$_2$ ligand was prepared according to literature.[26b] 219 mg (0.284 mmol) of [Et$_4$N]$_2$ *fac*-[Re(CO)$_3$Br$_3$] in 10 mL of CH$_2$Cl$_2$; 76 mg (0.275 mmol, 0.9 equiv.) of L$_2$ in 10 mL of CH$_2$Cl$_2$. Yield: 93 mg (52 %). Elemental Anal. Calcd. for C$_{20}$H$_{14}$BrN$_2$O$_3$ReS: C 38.22 %, H 2.25 %, N 4.46 %. Found: C 37.86 %, H 2.29 %, N 4.13 %. ^{1}H-NMR (400 MHz, CD$_2$Cl$_2$): δ (ppm) = 2.54 (s, 3H), 7.36 (t, J = 7.55 Hz, 1H), 7.43 (t, J =8.27 Hz, 1H), 7.48 (d, J = 7.91 Hz, 1H), 7.72 (d, J = 7.82 Hz, 1H), 7.90 (t, J = 8.06 Hz, 1H), 8.07–8.11 (m, 3H), 8.64 (d, J = 8.22 Hz, 1H), 8.89 (d, J = 9.43 Hz, 1H), 9.10 (s, 1H). IR (KBr pellet): $\nu_{C \equiv O}$ = 2017 cm-1, 1889 cm^{-1}. MLCT band (CH$_2$Cl$_2$) [ε (M^{-1} cm^{-1})]: 467 nm (2657). ESI-MS analysis (positive mode) m/z = 549.1 [M − Br]$^+$.

fac-[Mn(CO)$_3$L$_2$Br] L$_2$ = (Dipyrido[3,2-a:2′,3′-c]phenazine) (39): The L$_2$ ligand was prepared according to literature.[14] 30 mg (0.11 mmol) of L$_2$ and 91 mg (0.33 mmol, 3 equiv.) of [Mn(CO)$_5$Br] were placed in 50 mL of CH$_2$Cl$_2$. The solution was stirred overnight at room temperature while kept in the dark. A pure yellow solid was collected by filtration, washed with cold (0° C) solvent and dried under vacuum. Yield: 53 mg (32 %). Elemental Anal. Calcd. for

$C_{21}H_{10}BrMnN_4O_3$: C 50.33 %, H 2.01 %, N 11.18 %. Found: C 50.79 %, H 2.16 %, N 10.97 %. ^{1}H-NMR (400 MHz, CDCl$_3$): δ (ppm) = 8.04 (s, 4H), 8.44 (s, 2H), 9.64 (bs, 2H), 9.76 (d, J = 6.4 Hz, 2H). IR (KBr pellet): $\nu_{C\equiv O}$ = 2022 cm^{-1}, 1917 cm^{-1}. MLCT band (CH$_2$Cl$_2$) [ε (M^{-1} cm^{-1})]: 430 nm (4215). ESI-MS analysis (positive mode) m/z = 421.1 [M – Br]$^+$.

fac-[Mn(CO)$_3$L$_2$Br] L$_2$ = (6,6′-Diphenyl-4,4′-bipyrimidine) (41): The L$_2$ ligand was prepared according to reference[32]. 0.112 g (0.36 mmol) of L$_2$ and 300 mg (1.09 mmol, 3 equiv.) of [Mn(CO)$_5$Br] were added to 50 mL of CH$_2$Cl$_2$. The solution was stirred overnight at room temperature while kept in the dark. A pure dark red solid was collected by filtration, washed with cold (0° C) solvent and dried under vacuum. Yield: 162 mg (28 %). Elemental Anal. Calcd. for $C_{23}H_{14}BrMnN_4O_3$: C 52.20 %, H 2.67 %, N 10.59 %. Found: C 51.59 %, H 2.91 %, N 10.44 %. ^{1}H-NMR (400 MHz, [D$_6$]DMSO): δ (ppm) = 7.71–7.74 (m, 6H), 8.50–8.53 (m, 4H), 9.54 (s, 2H), 9.91 (s, 2H). IR (KBr pellet): $\nu_{C\equiv O}$ = 2034 cm^{-1}, 1950 cm^{-1}, 1901 cm^{-1}. MLCT band (CH$_2$Cl$_2$) [ε (M^{-1} cm^{-1})]: 512 nm (4000). ESI-MS analysis (positive mode) m/z = 449.1 [M – Br]$^+$ and 421.1 [M – Br – CO]$^+$.

fac-[Re(CO)$_3$L$_2$Br] L$_2$ = (6,6′-Diphenyl-4,4′-bipyrimidine) (42): The L$_2$ ligand was prepared according to literature.[32] The following reaction was carried out under argon. 138 mg (0.18 mmol) of [Et$_4$N]$_2$ fac-[Re(CO)$_3$Br$_3$] were dissolved in 10 mL of CH$_2$Cl$_2$. Then, 56 mg (0.18 mmol, 1 equiv.) of L$_2$ were added and the reaction mixture stirred at room temperature for 2 h. After this time a red solid had formed. This precipitate was collected by filtration, washed with cold (0° C) solvent and dried under vacuum. Yield: 56 mg (47 %). Elemental Anal. Calcd. for $C_{23}H_{14}BrN_4O_3Re$: C 41.82 %, H 2.14 %, N 8.48 %. Found: C 42.12 %, H 2.62 %, N 8.09 %. ^{1}H-NMR (400 MHz, CD$_2$Cl$_2$): δ (ppm) = 7.65–7.71 (m, 6H), 8.33 (m, 4H), 8.68 (s, 2H), 9.73 (s, 2H). IR (KBr pellet): $\nu_{C\equiv O}$ = 2016 cm^{-1}, 1885 cm^{-1}. MLCT band (CH$_2$Cl$_2$) [ε (M^{-1} cm^{-1})]: 467 nm (4740). ESI-MS analysis (positive mode) m/z = 581.1 [M – Br]$^+$.

fac-[Mn(CO)$_3$L$_2$Br] L$_2$ = (2,3-Di(pyridin-2-yl)quinoxaline) (43): The L$_2$ ligand was prepared according to literature.[33] 28 mg (0.1 mmol) of L$_2$ and 54 mg (0.2 mmol, 2 equiv.) of [Mn(CO)$_5$Br] were dissolved in 15 mL of CH$_2$Cl$_2$. The solution was stirred at reflux for 12 h while kept in the dark. After this time a dark violet compound was filtered from solution, washed with cold (0° C) solvent and dried under vacuum. Yield: 40 mg (28 %). Elemental Anal. Calcd. for $C_{24}H_{12}Br_2Mn_2N_4O_6$: C 39.92 %, H 1.68 %, N 7.76 %. Found: C 39.18 %, H 1.76 %, N 7.67 %. ^{1}H-NMR (400 MHz, CD$_2$Cl$_2$): δ (ppm) = 7.56 (t, J = 5.70 Hz, 2H), 7.87 (t, J = 8.07 Hz 2H), 8.15 (t, J = 5.31 Hz, 2H), 8.34 (d, J = 7.35 Hz, 2H), 8.79 (d, J = 4.53 Hz, 2H), 9.35 (d, J = 4.15 Hz, 2H). IR (KBr pellet): $\nu_{C\equiv O}$ = 2019 cm^{-1}, 1909 cm^{-1}. MLCT band (CH$_2$Cl$_2$) [ε (M^{-1} cm^{-1})]: 573 nm (3135). ESI-MS analysis (positive mode) m/z = 640.8 [M – Br]$^+$.

fac-[Re(CO)$_3$L$_2$Br] L$_2$ = (2,3-Di(pyridin-2-yl)quinoxaline) (44): The L$_2$ ligand was prepared according to literature.[33] The following reaction was carried out under argon. 153 mg (0.2 mmol) of [Et$_4$N]$_2$ fac-[Re(CO)$_3$Br$_3$] were dissolved in 40 mL of CH$_2$Cl$_2$. Then, 28 mg (0.1 mmol, 0.5 **equiv.**) of L$_2$ were added and the reaction mixture was stirred at reflux overnight. After hot filtration, the dark brown solid was dried and recrystallized from an acetone/ether mixture. Yield: 76 mg (39 %). Elemental Anal. Calcd. for $C_{24}H_{12}Br_2N_4O_6Re_2$: C 29.28 %, H 1.23 %, N 5.69 %. Found: C 31.08 %, H 1.75 %, N 5.44 %. ^{1}H-NMR (400 MHz, CD$_2$Cl$_2$): δ (ppm) = 7.61 (t, J = 6.60 Hz, 2H), 7.95 (dt, J = 8.00 Hz, 2H), 8.19–8.22 (m, 2H), 8.54 (d, J = 8.3 Hz, 2H), 8.72–8.75 (m, 2H), 9.19 (d, J = 5.42 Hz, 2H). IR (KBr pellet): $\nu_{C\equiv O}$ = 2036 cm^{-1}, 1895 cm^{-1}. MLCT band (CH$_2$Cl$_2$) [ε (M^{-1} cm^{-1})]: 543 nm (3700). ESI-MS analysis (positive mode) m/z = 903.0 [M – Br]$^+$. Single

crystals suitable for X-ray diffraction analysis were grown by slow evaporation of an acetone solution of 44.

fac-[Re(CO)$_3$L$_2$Br] L$_2$ = (5H-Cyclopenta[1,2-b:5,4-b′]dipyridin-5-one) (46): The L$_2$ ligand and complex **46** were prepared following the procedure described in literature[20] for the Mn complex with small variations. Briefly: a total of 84 mg (0.11 mmol) of [Et$_4$N]$_2$ fac-[Re(CO)$_3$Br$_3$] was dissolved in 5 mL of CH$_2$Cl$_2$. Then, 20 mg (0.1 mmol, 0.9 equiv.) of L$_2$ in 10 mL of CH$_2$Cl$_2$ were added dropwise under nitrogen. The reaction mixture was then stirred under nitrogen at room temperature overnight. At the end of the reaction, pentane was carefully layered on top of the yellow solution and the mixture was allowed to stand until crystals of 46 appeared. These were then filtered, dried and analyzed. Yield: 32 mg (54 %). Elemental Anal. Calcd. for $C_{14}H_6BrN_2O_4Re$: C 31.59 %, H 1.14 %, N 5.26 %. Found: C 31.57 %, H 1.15 %, N 5.40 %. ^{1}H-NMR (400 MHz, CDCl$_3$): δ (ppm) = 7.53–7.56 (m, 2H), 8.07–8.10 (m, 2H), 8.71–8.74 (m, 2H). IR (KBr pellet): $\nu_{C\equiv O}$ = 2017 cm^{-1}, 1889 cm^{-1}. MLCT band (CH$_2$Cl$_2$) [ε (M^{-1} cm^{-1})]: 400 nm (2820). ESI-MS analysis (positive mode) m/z = 344.9 [M – Br]$^+$. Single crystals suitable for X-ray diffraction analysis were grown by slow diffusion of pentane into a CH$_2$Cl$_2$ solution of **46**.

Synthesis of 6-Methyl-4,4′-bis(trifluoromethyl)-2,2′-bipyridine, L$_2$ of 47 and 48: 2-Chloro-6-methyl-4-(trifluoromethyl)pyridine (400 mg, 2.04 mmol, 1 equiv.), 2-tributylstannyl-4-(trifluoromethyl)pyridine[34] (1.03 g, 2.35 mmol, 1.13 equiv.) and Pd(PPh$_3$)$_4$ (118 mg, 0.1 mmol, 0.05 equiv.) were mixed in 35 mL of anhydrous toluene under argon and refluxed for 24 h. The crude mixture was concentrated under reduced pressure and dissolved in 20 mL HCl$_{aq.}$ 6 M. The aqueous phase was washed with 10 mL of ethyl acetate, then cooled to 0 °C, and neutralized with NH$_4$OH. The product was extracted from the aqueous solution with ethyl acetate (3 × 20 mL) and the combined organic phases were washed with Brine. The solvent was removed under rotary evaporation and the resulted yellow oil was used without further purification. Yield: 587 mg (94 %). NMR: ^{1}H-NMR (400 MHz, CD$_2$Cl$_2$): δ (ppm) = 8.88 (d, J = 5.13 Hz, 1H), 8.75 (s, 1H), 8.53 (s, 1H), 7.59–7.57 (m, 1H), 7.46 (s, 1H), 2.72 (s, 3H). ESI-MS analysis (positive mode) m/z = 329.1 [M + Na]$^+$.

fac-[Mn(CO)$_3$L$_2$Br] L$_2$ = (6-Methyl-4,4′-bis(trifluoromethyl)-2,2′-bipyridine) (47): The complex was obtained by a modification of a published procedure.[35] 34 mg (0.13 mmol, 1.5eq) of Mn(CO)$_5$Br and 26 mg (0.08 mmol, 1 equiv.) of L$_2$ were refluxed in dry diethyl ether (10 mL) overnight under argon atmosphere while kept in the dark. The solvent was removed under reduced pressure and the pure product was obtained through chromatography column on silica-gel with CH$_2$Cl$_2$ as eluent. Yield: 39 mg (94 %). Elemental Anal. Calcd. for $C_{16}H_8BrF_6MnN_2O_3$: C 36.60 %, H 1.54 %, N 5.34 %. Found: C 35.83 %, H 1.96 %, N 5.72 %. ^{1}H-NMR (400 MHz, CD$_2$Cl$_2$): δ (ppm) = 9.53 (d, J = 5.75 Hz, 1H), 8.38 (s, 1H), 8.25 (s, 1H), 7.80 (d, J = 5.75 Hz, 1H), 7.74 (s, 1H), 3.26 (s, 3H). IR (KBr pellet): $\nu_{C\equiv O}$ = 2026 cm^{-1}, 1916 cm^{-1}. MLCT band (CH$_2$Cl$_2$) [ε (M^{-1} cm^{-1})]: 463 nm (2710). ESI-MS analysis (positive mode) m/z = 445.3 [M – Br]$^+$.

fac-[Re(CO)$_3$L$_2$Br] L$_2$ = (6-Methyl-4,4′-bis(trifluoromethyl)-2,2′-bipyridine) (48): The compound was obtained by a modification of a published procedure.[36] To a solution of 132 mg (0.18 mmol, 1.1eq) of [Et$_4$N]$_2$ fac-[Re(CO)$_3$Br$_3$] in methanol (10 mL) was added dropwise L$_2$ (50 mg, 0.16 mmol, 1eq) dissolved in 2 mL of methanol. The reaction mixture was stirred overnight at 50 °C. At the end of the reaction the solution was filtered and the solvent was removed under reduced pressure. The crude was purified through chromatography column on SiO$_2$ with CH$_2$Cl$_2$ as eluent. Yield: 84 mg (80 %). Elemental Anal. Calcd. for $C_{16}H_8BrF_6N_2O_3Re$: C 29.28 %, H 1.23 %,

N 4.27 %. Found: C 30.01 %, H 1.57 %, N 4.55 %. ^{1}H-NMR (400 MHz, CD$_2$Cl$_2$): δ (ppm) = 9.35 (d, J = 5.77 Hz, 1H), 8.45 (s, 1H), 8.32 (s, 1H), 7.85 (s,1H), 7.81 (d, J = 5.77 Hz, 1H), 3.18 (s, 3H). IR (KBr pellet): $\nu_{C\equiv O}$ = 2018 cm^{-1}, 1889 cm^{-1}. MLCT band (CH$_2$Cl$_2$) [ε (M^{-1} cm^{-1})]: 427 nm (3215). ESI-MS analysis (positive mode) m/z = 576.9 [M − Br]$^+$.

fac-[Mn(CO)$_3$L$_2$Br] L$_2$ = (4-Methoxy-6-methyl-2,2′-bipyridine) (49): The L$_2$ ligand was prepared following the procedure described in literature.[37] The complex was obtained by a modification of a published procedure.[35] 34 mg (0.13 mmol, 1.5eq) of Mn(CO)$_5$Br and 16.5 mg (0.08 mmol, 1 equiv.) of L$_2$ were refluxed in dry diethyl ether (10 mL) for 4 h under argon atmosphere, until an orange precipitate was formed. The compound was filtered and used without further purification. Yield: 29 mg (87 %). Elemental Anal. Calcd. for C$_{15}$H$_{12}$BrMnN$_2$O$_4$: C 42.99 %, H 2.82 %, N 6.68 %. Found: C 43.22 %, H 2.93 %, N 6.21 %. ^{1}H-NMR (400 MHz, CD$_2$Cl$_2$): δ (ppm) = 9.27 (d, J = 5.13 Hz, 1H), 8.08–7.97 (m, 2H), 7.52–7.49 (m, 2H), 6.97 (s,, 1H), 3.98 (s, 3H), 3.06 (s, 3H). IR (KBr pellet): $\nu_{C\equiv O}$ = 2015 cm^{-1}, 1905 cm^{-1}. MLCT band (CH$_2$Cl$_2$) [ε (M^{-1} cm^{-1})]: 407 nm (2931). ESI-MS analysis (positive mode) m/z = 339.0 [M − Br]$^+$.

fac-[Re(CO)$_3$L$_2$Br] L$_2$ = (4-Methoxy-6-methyl-2,2′-bipyridine) (50): The complex was synthesized following the same procedure reported for complex **49**.[36] 92 mg (0.12 mmol, 1.2eq) of [Et$_4$N]$_2$ fac-[Re(CO)$_3$Br$_3$] in 10 mL of methanol and 20 mg of L$_2$ (0.1 mmol, 1eq) in 2 mL of methanol. Yield: 47 mg (85 %). Elemental Anal. Calcd. for C$_{15}$H$_{12}$BrN$_2$O$_4$Re: C 32.73 %, H 2.20 %, N 5.09 %. Found: C 32.65 %, H 2.28 %, N 4.99 %. ^{1}H-NMR (400 MHz, CD$_2$Cl$_2$): δ (ppm) = 9.09–9.07 (m, 1H) 8.15–8.13 (m, 1H), 8.08–8.03 (m, 1H), 7.56 (d, J = 2.70 Hz, 1H), 7.54–7.50 (m, 1H), 7.03 (d, J = 2.70, Hz, 1H), 4.00 (s, 3H), 2.99 (s, 3H). IR (KBr pellet): $\nu_{C\equiv O}$ = 2015 cm^{-1}, 1860 cm^{-1}. MLCT band (CH$_2$Cl$_2$) [ε (M^{-1} cm^{-1})]: 373 nm (3476). ESI-MS analysis (positive mode) m/z = 471.0 [M − Br]$^+$.

[1] a) S. Romanski, B. Kraus, U. Schatzschneider, J. M. Neudorfl, S. Amslinger, H. G. Schmalz, *Angew. Chem. Int. Ed.* **2011**, *50*, 2392–2396; *Angew. Chem.* **2011**, *123*, 2440–2444; b) S. Romanski, B. Kraus, M. Guttentag, W. Schlundt, H. Rucker, A. Adler, J. M. Neudorfl, R. Alberto, S. Amslinger, H. G. Schmalz, *Dalton Trans.* **2012**, *41*, 13862–13875; c) S. Botov, E. Stamellou, S. Romanski, M. Guttentag, R. Alberto, J. M. Neudorfl, B. Yard, H. G. Schmalz, *Organometallics* **2013**, *32*, 3587–3594.

[2] P. C. Kunz, H. Meyer, J. Barthel, S. Sollazzo, A. M. Schmidt, C. Janiak, *Chem. Commun.* **2013**, *49*, 4896–4898.

[3] a) F. Zobi, A. Degonda, M. C. Schaub, A. Y. Bogdanova, *Inorg. Chem.* **2010**, *49*, 7313–7322; b) F. Zobi, O. Blacque, R. A. Jacobs, M. C. Schaub, A. Y. Bogdanova, *Dalton Trans.* **2012**, *41*, 370–378; c) L. Prieto, J. Rossier, K. Derszniak, J. Dybas, R. M. Oetterli, E. Kottelat, S. Chlopicki, F. Zelder, F. Zobi, *Chem. Commun.* **2017**, *53*, 000–000; d) B. J. Aucott, J. S. Ward, S. G. Andrew, J. Milani, A. C. Whitwood, J. M. Lynam, A. Parkin, I. J. S. Fairlamh, *Inorg. Chem.* **2017**, *56*, 5431–5440; e) R. Motterlini, P. Sawle, S. Bains, J. Hammad, R. Alberto, R. Foresti, C. J. Green, *Faseb J.* **2004**, *18*, 284–286; f) T. S. Pitchumony, B. Spingler, R. Motterlini, R. Alberto, *Chimia* **2008**, *62*,

277–279; g) T. S. Pitchumony, B. Spingler, R. Motterlini, R. Alberto, *Org. Biomol. Chem.* **2010**, *8*, 4849–4854.

[4] a) A. A. Ahanger, S. Prawez, D. Kumar, R. Prasad, Amarpal, S. K. Tandan, D. Kumar, *Naunyn-Schmiedebergs Arch. Pharmakol.* **2011**, *384*, 93–102; b) R. Motterlini, B. Haas, R. Foresti, *Med. Gas Res.* **2012**, *2*, 28.

[5] a) E. Kottelat, F. Zobi, *Inorganics* **2017**, *5*, 24–43; b) M. A. Wright, J. A. Wright, *Dalton Trans.* **2016**, *45*, 6801–6811.

[6] a) E. Kottelat, A. Ruggi, F. Zobi, *Dalton Trans.* **2016**, *45*, 6920–6927; b) S. J. Carrington, I. Chakraborty, P. K. Mascharak, *Chem. Commun.* **2013**, *49*, 11254–11256; c) S. J. Carrington, I. Chakraborty, P. K. Mascharak, *Dalton Trans.* **2015**, *44*, 13828–13834; d) M. A. Gonzales, P. K. Mascharak, *J. Inorg. Biochem.* **2014**, *133*, 127–135.

[7] a) S. J. Carrington, I. Chakraborty, J. M. L. Bernard, P. K. Mascharak, *Inorg. Chem.* **2016**, *55*, 7852–7858; b) A. E. Pierri, A. Pallaoro, G. Wu, P. C. Ford, *J. Am. Chem. Soc.* **2012**, *134*, 18197–18200; c) S. C. Marker, S. N. MacMillan, W. R. Zipfel, Z. Li, P. C. Ford, J. J. Wilson, *Inorg. Chem.* **2018**, *57*, 1311–1331.

[8] I. Chakraborty, S. J. Carrington, P. K. Mascharak, *ChemMedChem* **2014**, *9*, 1266–1274.

[9] a) H. Takeda, O. Ishitani, *Coord. Chem. Rev.* **2010**, *254*, 346–354; b) J. L. White, M. F. Baruch, J. E. Pander, Y. Hu, I. C. Fortmeyer, J. E. Park, T. Zhang, K. Liao, J. Gu, Y. Yan, T. W. Shaw, E. Abelev, A. B. Bocarsly, *Chem. Rev.* **2015**, *115*, 12888–12935.

[10] a) F. L. Thorp-Greenwood, R. G. Balasingham, M. P. Coogan, *J. Organomet. Chem.* **2012**, *714*, 12–21; b) V. Fernandez-Moreira, F. L. Thorp-Greenwood, M. P. Coogan, *Chem. Commun.* **2010**, *46*, 186–202; c) M. P. Coogan, V. Fernandez-Moreira, *Chem. Commun.* **2014**, *50*, 384–399.

[11] A. Leonidova, G. Gasser, *ACS Chem. Biol.* **2014**, *9*, 2180–2193.

[12] I. Chakraborty, S. J. Carrington, P. K. Mascharak, *Acc. Chem. Res.* **2014**, *47*, 2603–2611.

[13] See ref. [8].

[14] P. Kurz, B. Probst, B. Spingler, R. Alberto, *Eur. J. Inorg. Chem.* **2006**, *2006*, 2966–2974.

[15] A. B. P. Lever, *Inorg. Chem.* **1990**, *29*, 1271–1285.

[16] a) F. Zobi, *Inorg. Chem.* **2009**, *48*, 10845–10855; b) F. Zobi, *Inorg. Chem.* **2010**, *49*, 10370–10377.

[17] C. J. Kleverlaan, F. Hartl, D. J. Stufkens, *J. Organomet. Chem.* **1998**, *561*, 57–65.

[18] B. D. Rossenaar, D. J. Stufkens, A. Vlcek, *Inorg. Chim. Acta* **1996**, *247*, 247–255.

[19] D. A. Kurtz, B. Dhakal, R. J. Hulme, G. S. Nichol, G. A. N. Felton, *Inorg. Chim. Acta* **2015**, *427*, 22–26.

[20] J. Jimenez, I. Chakraborty, P. K. Mascharak, *Eur. J. Inorg. Chem.* **2015**, *2015*, 5021–5026.

[21] S. A. Moya, J. Guerrero, R. Pastene, I. Azocar-Guzman, A. J. Pardey, *Polyhedron* **2002**, *21*, 439–444.

[22] S. A. Moya, J. Guerrero, R. Pastene, R. Schmidt, R. Sariego, R. Sartori, J. Sanzaparicio, I. Fonseca, M. Martinezripoll, *Inorg. Chem.* **1994**, *33*, 2341–2346.

[23] G. J. Stor, S. L. Morrison, D. J. Stufkens, A. Oskam, *Organometallics* **1994**, *13*, 2641–2650.

[24] B. D. Rossenaar, D. J. Stufkens, A. Vlcek, *Inorg. Chem.* **1996**, *35*, 2902–2909.

[25] B. D. Rossenaar, F. Hartl, D. J. Stufkens, C. Amatore, E. Maisonhaute, J. N. Verpeaux, *Organometallics* **1997**, *16*, 4675–4685.

[26] a) S. E. A. Lumsden, G. Durgaprasad, K. A. T. Muthiah, M. J. Rose, *Dalton Trans.* **2014**, *43*, 10725–10738; b) M. A. Gonzalez, S. J. Carrington, N. L. Fry, J. L. Martinez, P. K. Mascharak, *Inorg. Chem.* **2012**, *51*, 11930–11940.

[27] See ref. [20].

[2] F. Herman, S. Skillman, *Atomic Structure Calculations* **1963**, Prentice-Hall Inc., New Jersey.

[29] V. Bewick, L. Cheek, J. Ball, *Crit. Care* **2003**, *7*, 451–459.

[30] G. M. Sheldrick, *Acta Crystallogr., Sect. A* **2015**, *71*, 3–8.

[31] G. M. Sheldrick, *Acta Crystallogr., Sect. C* **2015**, *71*, 3–8.

[32] E. Ioachim, E. A. Medlycott, M. I. J. Polson, G. S. Hanan, *Eur. J. Org. Chem.* **2005**, *2005*, 3775–3780.

[33] a) Y. J. Cho, S. Y. Kim, M. Cho, K. R. Wee, H. J. Son, W. S. Han, D. W. Cho, S. O. Kang, *Phys. Chem. Chem. Phys.* **2016**, *18*, 15162–15169; b) J. H. Shen, X. D. Wang, X. Lin, Z. H. Yang, G. L. Cheng, X. L. Cui, *Org. Lett.* **2016**, *18*, 1378–1381.

[34] S. Aroua, T. K. Todorova, P. Hommes, L. M. Charnoreau, H. U. Reissig, V. Mougel, M. Fontecave, *Inorg. Chem.* **2017**, *56*, 5930–5940.

[35] Z. Li, A. E. Pierri, P. J. Huang, G. Wu, A. V. Iretskii, P. C. Ford, *Inorg. Chem.* **2017**, *56*, 6094–6104.

[36] M. Schutte, G. Kemp, H. G. Visser, A. Roodt, *Inorg. Chem.* **2011**, *50*, 12486–12498.

[37] J. Dash, H. U. Reissig, *Chem. Eur. J.* **2009**, *15*, 6811–6814.